IEEE Access
Multidisciplinary | Rapid Review | Open Access Journal

Received March 19, 2021, accepted April 7, 2021, date of publication April 13, 2021, date of current version April 22, 2021.

Digital Object Identifier 10.1109/ACCESS.2021.3072969

A Demand-Supply Matching-Based Approach for Mapping Renewable Resources Towards 100% Renewable Grids in 2050

LOIY AL-GHUSSAIN[1], ADNAN DARWISH AHMAD[2], AHMAD M. ABUBAKER[2], MOHAMMAD ABUJUBBEH[3], ABDULAZIZ ALMALAQ[4], (Member, IEEE), AND MOHAMED A. MOHAMED[5,6], (Member, IEEE)

[1]Mechanical Engineering Department, University of Kentucky, Lexington, KY 40506, USA
[2]Institute of Research for Technology Development (IR4TD), University of Kentucky, Lexington, KY 40506, USA
[3]Department of Electrical and Computer Engineering, Kansas State University, Manhattan, KS 66506, USA
[4]Department of Electrical Engineering, University of Hail, Hail 81451, Saudi Arabia
[5]Electrical Engineering Department, Faculty of Engineering, Minia University, Minia 61519, Egypt
[6]Department of Electrical Engineering, Fuzhou University, Fuzhou 350116, China

Corresponding authors: Loiy Al-Ghussain (loiy.al-ghussain@uky.edu), Adnan Darwish Ahmad (adnandarwish@uky.edu), and Mohamed A. Mohamed (dr.mohamed.abdelaziz@mu.edu.eg)

ABSTRACT Recently, many renewable energy (RE) initiatives around the world are based on general frameworks that accommodate the regional assessment taking into account the mismatch of supply and demand with pre-set goals to reduce energy costs and harmful emissions. Hence, relying entirely on individual assessment and RE deployment scenarios may not be effective. Instead, developing a multi-faceted RE assessment framework is vital to achieving these goals. In this study, a regional RE assessment approach is presented taking into account the mismatch of supply and demand with an emphasis on Photovoltaic (PV) and wind turbine systems. The study incorporates mapping of renewable resources optimized capacities for different configurations of PV and wind systems for multiple sites via test case. This approach not only optimizes system size but also provides the appropriate size at which the maximum renewable energy fraction in the regional power generation mix is maximized while reducing energy costs using MATLAB's ParetoSearch algorithm. The performance of the proposed approach is tested in a realistic test site, and the results demonstrate the potential for maximizing the RE share compared to the achievable previously reported fractions. The results indicate the importance of resource mapping based on energy-demand matching rather than a quantitative assessment of anchorage sites. In the examined case study, the new assessment approach led to the identification of the best location for installing a hybrid PV / wind system with a storage system capable of achieving a nearly 100% autonomous RE system with Levelized cost of electricity of 0.05 USD/kWh.

INDEX TERMS Renewable energy resources, multi-objective optimization, energy demand matching, resources assessment, resources geographical mapping.

I. INTRODUCTION

Recently, the energy market witnessed a significant decline in the adaptation of distributed energy resources (DERs) such as wind turbines and solar Photovoltaics (PV) due to the impacts of the novel COVID-19 on the world's economy. With the global crisis, energy demand has dropped down in the industrial and commercial sectors, in contrary, the load increased in the residential sector. Therefore, governments had to put new strategies to tackle down the ongoing challenges. Elavarasan *et al.* [1] studied the impact of COVID-19 pandemic on the power sector for the Indian power grid. Their work investigated global scenarios along with the social-economic and technical issues encountered by utilities.

According to [2], 40% of the RE integration plans in 2020 were suspended. Yet, the same article emphasizes that the economic advantages of clean energy production methods possess a long-term value compared to fossil-fuel-based

The associate editor coordinating the review of this manuscript and approving it for publication was Dipankar Deb.

methods. This in return increases the stress on renewable energy (RE) sources and therefore, the expected share of DERs in the existing power generation mix is expected to increase dramatically. Besides, projections suggest that prices of producing electric power through clean energy sources, wind, and PV for instance, are expected to significantly decay in the upcoming decades [3]. Nevertheless, the inclusion of RE in a nation's economic advancement strategy is predominantly a choice that depends greatly on decision-makers to recover the country's economy.

With the promising foresight on the world's industry plans to reopen and get back to the normal way of life, the energy demand is expected to rapidly increase to meet the new stress on energy consumption as the impact of the pandemic fades gradually. Purposefully, countries will investigate alternatives to meet this demand. Conventionally, fossil fuels were dominant and took the larger portion of the power generation mix. Yet, the fossil fuel-based methods are fragile as their supply chain is not reliable during harsh conditions such as wars and pandemics. Moreover, fossil fuel resources are depleting and therefore the shift toward a more robust and profound means of energy production is essential.

Jordan (30.5852° N, 36.2384° E) among the developing countries, with no exception, is facing many struggles to cover its domestic energy demands, in which around 94% of the country's demand is imported from neighboring countries [4]. Furthermore, the country faced two major catastrophic power events one of which is due to the disturbance of oil supply during the Iraqi war in 2003 and the other is during 2011 as a result of the revolution in Egypt [5]. This instability in oil prices and the continuous disruptions in imported oil motivated the country to investigate alternative energy sources that are environmentally friendly, reliable, and meet the demand of the county independently, such as renewables, at acceptable rates of generation [6]. Moreover, the energy demand growth rate in developing countries is around 5%, which is greater than that of developed countries, 1% [7]. Therefore, developing countries will need more energy supplies as the industrial sector is growing. Essentially, the most important turning points in the fight against climate change, the Kyoto Protocol and the Paris agreement [4] forced stakeholders to take action and keep the world temperature increase below 2 °C. This goal can be accomplished by taking into action the investments and regulatory frameworks that are necessary for low carbon emissions while meeting the increased demand. Jordan enforced a plan to meet 10 % of their energy demand by DERs, including PVs, wind turbines, and biomass resources while keeping the harmful emissions as low as possible and help to advance the economy of the country by 2020 [8]. Few projects in the country were successfully installed with varying capacities of 407 MW of wind and 670 MW of solar photovoltaics by 2015 [5]. Nevertheless, future energy planning should be diverse enough to accommodate more capacities, not only for minimizing demand-supply mismatches, but also considering a generic framework that considers all the characteristics in the proposed RE approach [9]. In other words, it is of utmost importance to enforce a careful energy planning scheme that relies on pre-implementation strategies, including data collection, analysis, and evaluation of the desired site in the country, which will in return enable extracting the maximum benefits of this integration [10], [11]. Subsequently, the necessary circumstances can be created for a given future target, say 100% RE, and the energy plan can be kept under revision and constant estimation to adapt to the changing conditions in the region [12]. Many research efforts [13]–[16] attempted to study the long-term plans of RE integration to ensure a smooth and feasible switch to 100% RE environments. Authors [17] proposes a new approach that considers hourly-based simulations to determine the structure of a flexible energy market taking into account external energy exchanges on an international scale. This study proves that the transition toward a 50% RE-based market is possible based on sensitivity and socioeconomic analysis. Another study in [18] investigated the long-term plans in France taking into account the short-term grid dynamics. The study concludes that a portion of 65 % RE could help the stability of the electric grid with a reliable supply.

Solar photovoltaics and wind turbines are the most widely used RE sources in the existing body of literature [19]–[22]. Their abundance and comparatively lower costs make them superior to other RE sources such as hydrothermal, biothermal, and tidal waves [23]. For this reason, many research articles focus on solar photovoltaics and wind turbines as the input to their energy plans [24]–[26]. Studies [27]–[29] relied on solar power for energy production, water desalination, and cooling fluids. The study [30] for instance, investigated the possibility of replacing conventional fossil-fuel generations with solar-based energy systems. Additionally, wind power prediction has been investigated thoroughly in the body of literature [31]–[33]. New hybrid energy systems are also proposed in the literature that utilizes wind or solar energy as a backup generator that can be coupled with centralized power plans [34], geothermal [35], piezoelectric [36] to enhance the reliability of the produced power.

The hybridization of both solar photovoltaics and wind turbines is proved to provide more stable and reliable power outputs when compared to standalone operations [37]. Furthermore, the hybridization provides lower installation, as well as production costs since the installed capacity of each unit, is smaller relative to stand-alone integration [38], [39]. The optimization of RESs in the last decade has gained significant interest by researchers due to its vital role in affecting the technical and economic feasibilities of RESs. Hence, various optimization techniques have been developed and proposed for achieving the maximum economic and technical feasibilities [40]–[43]. For instance, reference [44] investigated the feasibility of a renewable energy system (RES) comprised of PV, wind turbines, and storage systems (ESS) to cover the demand for base loads of Chile. The study included an optimization approach to optimally size the components of the system considering the weather conditions. This study

further considers different comparison scenarios between different locations in the country. The study confirmed that there is a high potential in RE generation and stored capacities, which can be sold back to the grid assuming there exist net-metering programs [10], [45].

The mismatch between demand and energy supplied is one of the barriers to the vast deployment of RES, in the last decade, many researchers tried to overcome this issue by the integration of ESS [41], identifying the areas that have the maximum RE resources [46], [47], assessing the availability and the synergy of solar and wind resources [48], [49] or by the implementation of load management strategies [50], [51]. The previous studies in the literature presented the best location for the installation of the RES based on either the quantity of the resources or the availability of it without investigating the possibility of matching the local demand by the RES. The assessment methodologies of the RE resources in the literature lead to improper utilization of the RE resources and would be a barrier toward achieving 100% autonomous RE grids. Hence it is important to investigate the capability of the RE supply to meet the local energy demand as part of the energy resources assessment in any location.

Recent studies identified the techno-economic evaluation of hybrid RE systems. Shafiullah [52] studied a hybrid renewable energy integration consisting of solar and wind forecasting in advance in subtropical climate of Central Queensland. His study showed techno-economic and environmental prospects of renewable energy. Results indicated that subtropical climatic has substantial capabilities, in which energy generation cost and global warming would be reduced. Yue *et al.* [15] pointed out that the studies of the 100 % renewable energy systems focuses on the power sector using exploratory methods. In their work, they considered a whole system approach and exploring optimal pathways approach towards 100 % renewable energy by 2050. Elavarasan *et al.* [53] conducted a comprehensive review regarding the challenges and policies of renewable energy of the Indian states. Their work discussed in depth the transition to renewable energy for three states. Shoeb and Shafiullah [54] used renewable energy in order to provide energy for irrigation purposes in rural areas. Azzuni *et al.* [16] developed a policy scenario for Jordan to transform the energy system to 100 % renewable energy. Also, they analyzed how the energy security is enhanced as a result. They have used the LUT energy system transition model to explore the feasibility of the transition. The LUT is an optimization tool which defines the structure of the optimal cost-energy system influenced by financial assumptions. Optimization was carried out in two steps. The first step is matching between the demand and supply in hourly resolution, where the demand comes from the residential, commercial, and industry sector and the supply is the PV and battery storage plus individual heating capacities. The demand by the sectors is limited to 20 % of the total demand by 2050. In the second step, the met demand for all sectors must be in every hour of the applied year. Additionally, the installed capacity if the RE is constrained to a maximum of 20 % growth in every 5 years' time step until achieving 100 % by 2050.

Based on the analyzed literature, it can be seen that investigations of standalone or hybrid renewable-energy systems were previously based on installation in energy-rich sites rather than sites of highest matching. When researchers investigated a renewable energy system, installation sites were usually assessed based on the solar or wind energy density of those sites, and the economic assessment followed to address the issue of feasibility of the corresponding installation capacities. However, sites of high energy resources might not necessarily resemble sites of high demand-matching; a result of the intermittent nature of the renewable energy resources which creates a mismatch between the demand and supply profiles. This means that a site with high wind resources, where the bulk of energy is allocated at a time of low demand might lead to less demand matching, as compared to another site with lower resources but a better matching. In this work, we demonstrated that assessing solar and wind RESs and corresponding installation-capacities based on maps of energy densities; for instance, solar insolation or average wind-speed maps is not optimal, and therefore, mapping based on demand-supply matching was introduced instead. This approach, as shown for the case of Jordan, resulted in an RES fraction of 90.6% without an energy storage system, compared to previously reported maximum of 70% [5]. Although Jordan was used as a case study in our work to demonstrate the superiority of the approach, this mapping technique could be extrapolated following the methodology presented in the next section to any other country, to enhance the achievable RES fraction based on their energy resources supply-demand matching profile, hence, increasing the renewable penetration in the electrical grids worldwide by the year 2050.Developing such assessment approaches paves the way for maximum utilization of wind and solar resources and contributes to the movement toward green societies. Therefore, the main contributions of this paper can be listed as follows:

- A mapping approach for assessing the solar and wind energy resources based on the matching between the demand and the supply is presented.
- The optimal RES capacities with and without ESS were found at each location using multi-objective optimization based on maximizing the contribution of RES to local demand and the demand-supply fraction while minimizing the cost of supplied energy, to assess the advantage of the presented mapping.
- Mapping the performance of the optimal capacities of six RES configurations considering a real-world test system, in this work Jordan noting that this methodology can be applied to any location of a known demand and supply profiles to maximize the RES fractions and enhance the renewable penetration in electrical grids by 2050.

II. METHODOLOGY AND SYSTEM DESIGN: RESOURCE ASSESSMENT AND OPTIMIZATION

The authors here acknowledge the importance of renewable energy penetration models and policies for comparison and design of a country's transition plan to a 100% renewable grid. That said, we would like to stress an important point, that is the goal of our work was not to develop a plan for Jordan's renewable energy transition but to use Jordan as a case study to show that a map of renewable-resources-matching profile is superior to conventional maps based on renewable energy densities when it comes to estimation of the achievable RES fraction and the required RES installation capacities. The planning for a 100% transition in Jordan under different proposed scenarios was studied by researchers like Kiwan *et al.* in 2020, whose work has been included in our literature and results sections; to show the advantages of the proposed demand-supply matching mapping approach as compared to the previous methods. Jordan doesn't import nor export as seen in [55]. However, excess energy generated by the renewable energy would be sold to the neighbor countries in the future [56]. The rate of selling is assumed to be 0.05 USD/kWh which is the same as the current cost rate. Existing power plants are considered to work as backups when shortages occur.

Energy generated by the PV and wind models is the main parameter to assess the RES potential at different locations. Hence, in this section, the estimation of the hourly power generated by the PV and wind methodology is presented, and then followed by setting the energy flow logic, and finally, the methodology used to assess the economic feasibility of the systems is presented.

A. SOLAR PHOTOVOLTAIC PLANT

1) SYSTEM GEOMETRICAL CONSIDERATIONS

For a given region, one can estimate the energy that can be obtained through a PV system by evaluating the solar data of that region. This involves analyzing several parameters associated with the location such as solar and surface azimuth, tilt, and zenith angles as well as the earth's declination and latitude. For the present study, we estimate the aforementioned parameters based on a method proposed in reference [57], which is also described in this article.

Solar energy evaluation mainly depends on what is known as the hour angle, in degrees, which can be represented as the angular displacement between the surface of the sun and the observer's meridian. One can have a negative or positive displacement, depending on the earth's rotations about its axis, during daytime and nighttime, respectively as follow:

$$\omega = (t_s - 12) \times 15 \tag{1}$$

$$\mathrm{t_s} = \mathrm{t_{std}} + 4 \times (\mathrm{L_{st}} - \mathrm{L_{loc}}) + \mathrm{E} \tag{2}$$

$$\mathrm{L_{st}} = \begin{cases} -\mathrm{T_z} \times 15, & \mathrm{T_z} \leq 0 \\ 360 - \mathrm{T_z} \times 15, & \mathrm{T_z} > 0 \end{cases} \tag{3}$$

$$\mathrm{L_{loc}} = \begin{cases} \mathrm{L_{loc}}, & \text{if } \mathrm{L_{loc}} \text{ in the West} \\ 360 - \mathrm{L_{loc}}, & \text{if} \mathrm{L_{loc}} \text{ in the East} \end{cases} \tag{4}$$

The estimation of energy output by solar photovoltaic systems depends on another essential parameter, known as solar time, which can be represented by the position of the sun in the sky. Initially, one must convert from local to solar time by a correction factor of 4 minutes considering each singular degree difference in the declination between the standardized meridian and the region declination as follows:

$$\begin{aligned} \mathrm{E} = 229.2 \times (&0.000075 + 0.001868 \\ &\times \cos \mathrm{B} - 0.032077 \\ &\times \sin \mathrm{B} - 0.014615 \times \cos (2 \times \mathrm{B}) \\ &-0.04089 \times \sin (2 \times \mathrm{B})) \end{aligned} \tag{5}$$

where,

$$\mathrm{B} = (n - 1) \times \frac{360}{365} \tag{6}$$

Now, one can calculate the azimuth angle using (7) as the positioning of the sun taking the true south as the reference point, which varies between −180 and 180 degrees. For this, we assume prior knowledge of the site latitude, surface declination angle, as well as zenith angle [57]. Here, solar azimuth and hour angle have the same sign. Finally, the incidence angle for the solar system can be calculated considering the surface zenith, tilt, hour, and solar azimuth angles using (10).

$$\gamma_s = \text{sign}\,(\omega) \times \left| \cos^{-1}\left(\frac{\cos\theta z \sin\phi - \sin\delta}{\sin\theta z \cos\phi}\right) \right| \tag{7}$$

where,

$$\cos\theta z = \cos\phi \cos\delta \cos\omega + \sin\phi \sin\delta \tag{8}$$

$$\delta = 23.45 \times \sin\left(360 \times \frac{284 + \mathrm{n}}{365}\right) \tag{9}$$

$$\cos\theta = \cos\theta z \cos\beta + \sin\theta z \sin\beta \cos(\gamma_s - \gamma) \tag{10}$$

2) SOLAR IRRADIATION

This subsection deals with estimating the solar insolation for a tilted surface by evaluating two segments of insolation, namely, beam and diffusion. One can calculate the standard normal irradiation based on estimating the vertical portion of the beam type insolation on that tilted surface. As for later segments of the insolation, diffusion type, in this work, the isotropic sky model is employed, which predicts an equivalent scatter magnitude in all outgoing directions. Then, the surface tilt, as well as the sky-dome factor, helps to calculate the diffuse insolation that is irradiated on the surface by the sun as follows,

$$I_{b,t} = I_{b,n} \times \cos\theta \tag{11}$$

$$I_{d,t} = I_d \times \left(\frac{1 + \cos\beta}{2}\right) \tag{12}$$

$$I_T = I_{b,t} + I_{d,t} \tag{13}$$

It should be noted that this study uses the ambient temperature, and hourly diffuse and direction insolation data for

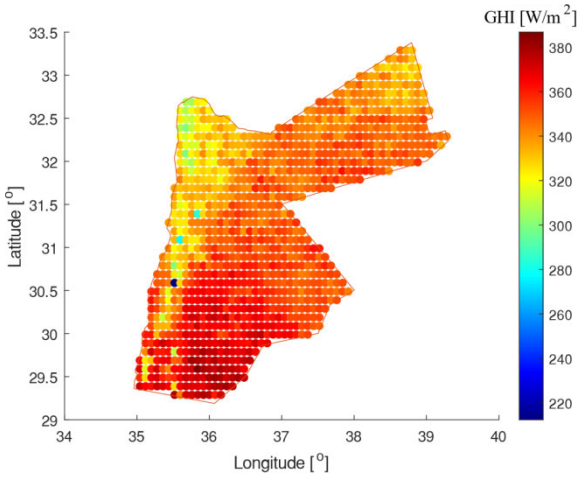

FIGURE 1. Geographical map of the average hourly global horizontal insolation in Jordan.

a standard meteorological year (TMY) as provided by the PVGIS software, Fig. 1 shows the average hourly TMY-GHI of Jordan. The next subsection highlights the specifications of the PV plant as well as the relative energy output.

3) PV PLANT ENERGY OUTPUT

Based on solar insolation calculations in the previous subsection, one can calculate the power produced by the PV plant as follows,

$$E_{PV} = \eta_{PV} \times I_T \times \mathrm{A_m} \times \mathrm{N_m} \times PR \tag{14}$$

where,

$$\eta_{PV} = \eta_{\mathrm{PV,Ref}} \times (1 - \beta_{\mathrm{Ref}} \times (T_{PV} - \mathrm{T_{Ref,STC}})) \tag{15}$$

$$T_{PV} = T_{amb} + (\mathrm{NOCT} - \mathrm{T_{Ref,NOCT}}) \times \frac{I_T}{\mathrm{I_{Ref}}} \tag{16}$$

Here, it is assumed that PR is 0.85; which accounts for some system's losses such as inverter and wiring losses as well as losses due to shading. It is also assumed in this work that all the modules in the PV plants will have the same cell temperature and efficiency. Accordingly, the modules are expected to receive an equivalent amount of solar irradiation. The solar modules used in this work are based on CS3L-365 design by Canadian Solar, where Table 1 illustrates the technical specifications.

B. WIND TURBINE ENERGY OUTPUT

This subsection presents the assessment of the wind resources in the region. The geographical conditions and the associated wind speeds of the sites are essential when analyzing the wind turbine output energy. The fact that wind speeds are fluctuating naturally due to weather conditions of the site means that the turbine energy output will be accordingly intermittent. Thus, it is vital to take rely on data analytics of the location to avoid under or over prediction of the wind speeds. This study utilizes the hourly TMY data, provided by PVGIS software, which includes wind speeds at a standardized test height,

TABLE 1. PV modules technical parameters.

Parameter	Value
Output power (W)	365
Module reference efficiency (%)	19.7
The module temperature coefficient (1/°C)	0.0036
The temperature of module* (°C)	25
The cell nominal operating temperature (°C)	42
Reference module temperature* (°C)	20
Reference insolation* (W/m^2)	800
Module area (m^2)	1.85

*: recorded at standard/nominal test conditions

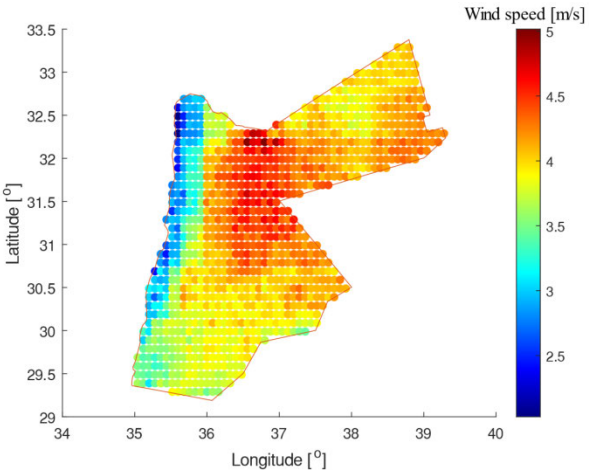

FIGURE 2. Geographical map of the average hourly wind speed at ground level in Jordan.

10 m above ground level. Fig. 2 shows the average hourly wind speeds in Jordan.

This data is further corrected according to wind turbine hub height based as follow:

$$u_Z = u_1 \times \left(\frac{\mathrm{Z}}{\mathrm{Z_1}}\right)^{\alpha} \tag{17}$$

Here, α is taken as 1/7 [5]. In this study, the power generation of the wind turbines is assumed to be uniform according to the hourly wind speed Weibull distribution. Accordingly, the hourly electric power generation of the wind turbines can be computed as in (18), where it is assumed that the wind turbines are operated with two constraints on their shaft speeds. Namely, a minimum cut-in speed required for the turbines to start producing power, and a cut-off speed that ensures safe operation at which the turbines are shut down to avoid abnormal performance.

$$P_e = \begin{cases} 0, & u_Z < \mathrm{u_C or} u_Z > \mathrm{u_F} \\ \mathrm{a} + \mathrm{b} \times (u_Z)^{\mathrm{K}}, & \mathrm{u_c} \le u_Z \le \mathrm{u_R} \\ \mathrm{P_{e,R}}, & \mathrm{u_R} < u_Z \le \mathrm{u_F} \end{cases} \tag{18}$$

Here, a and b are computed as follows:

$$a = P_{e,R} \times \frac{(u_C)^K}{(u_C)^K - (u_R)^K} \tag{19}$$

$$b = \frac{P_{e,R}}{(u_R)^K - (u_C)^K} \tag{20}$$

where,

$$K = \left(\bar{\sigma_u}\right)^{-1.086}, 1 \leq K \leq 10 \tag{21}$$

$$E_{wind} = N \times P_e \tag{22}$$

C. ENERGY DEMAND AND STORAGE SYSTEMS

The natural variability of RE sources creates an undesirable fluctuation in their power outputs and therefore, rising system instability issues. This is because the operations in power systems become weaker with the introduction of such non-dispatchable resources. To overcome this issue, typically different RE sources are hybridized to ensure a somewhat stable power output. Yet, this is not generally an optimal solution considering the time difference in peak power generation by the sources. For instance, it is known that PV systems have the highest power output during the daytime, at which the load can be less intense. Whereas for wind energy systems; their peak energy outputs are experienced during the evenings or nighttime. Therefore, to overcome this problem, new research motivates the usage of ESS as a way of overcoming the demand-supply mismatch at times of deficit power output by the RES.

In this work, four scenarios are created to compare the effectiveness of the method and identify the optimal mix that maximally meets the demand with the highest renewable energy fraction. The scenarios include a hybrid RES in one site with and without a coupled ESS and a hybrid RES scattered among different sites with and without a coupled ESS. The next subsections highlight the algorithm used in this study for both cases, with and without an ESS:

1) ON-GRID RES WITHOUT ESS

The first scenario is comprised of a hybrid energy system that is linked to the utility network to guarantee the availability of energy at times when demand is not met by the RES. Firstly, the demand is met by the RES and if there exists a deficit in covering the demand instantly, the supply is switched to the grid. Excess power generated by the RES will be fed back to the utility network [41]. The energy dispatch strategy that elaborates this methodology was adopted from [58].

2) ON-GRID RES WITH ESS

Similar to the previous case, the present setup is connected to the utility grid. However, an ESS is coupled with a hybrid energy system. The storage system in this study uses a Lithium-Ion battery for accommodating the excess energy generated by the RES. Among different battery types in literature, the Lithium-Ion battery has been chosen for its efficiency, portability, and large energy to weight ratio [30]. The round-trip efficiency, as well as the depth of discharge, are used to set up the energy model in this work where the Lithium-Ion battery round-trip efficiency and depth of discharge were assumed to be 95% and 60%, respectively as reported in [31]. When the RES generates excess energy, it will be collected in the storage system to be utilized later for covering the increased demand. If the stored energy still does not fully meet the demand, then the deficit in supply is met by the utility grid [41]. In cases where there is a large energy surplus, larger than the storage system can accommodate, then it will be fed back to the utility grid. The energy flow chart that illustrates the on-grid RES flowchart coupled with an energy storage facility can be found in [58].

D. ECONOMIC FEASIBILITY EVALUATION

The adaptation of RE sources into the present generation mixes relies not only on the technical feasibility but also on the economic profitability of the investment. A complete techno-economic feasibility analysis is therefore implemented in this study. The analysis is based on standardized project assessment indicators such as the (PBP), (LCOE), and (NPV). The analysis considers the installation cost of each unit included in the hybrid energy system involving a battery storage facility. The operation and maintenance costs are also a part of this analysis. The economic parameters of the installation can be estimated as follows:

$$LCOE = \frac{C_i + \sum_{t=1}^{LT} \frac{M_t}{(1+r)^t}}{\sum_{t=1}^{LT} \frac{D_{RES}}{(1+r)^t}} \tag{23}$$

$$PBP = \frac{C_i}{R_{t1}} \tag{24}$$

$$NPV = \sum_{t=1}^{LT} \frac{R_t}{(1+r)^t} - C_i \tag{25}$$

where,

$$C_i = C_{PV} + C_{WT} + C_{ESS} \tag{26}$$

Note that surplus electricity is sold to neighboring countries. The selling rate is assumed to be the same as the cost of electricity generation. The respective economic elements of the system are shown in Table 2.

E. PERFORMANCE INDICATORS OF THE RES

For the analysis, a typical Jordanian hourly energy demand profile in 2017 (the most recent record) is adapted from the Jordanian Electrical Power Company (JEPCO). Subsequently, this hourly demand curve is used to create an hourly load profile for a typical consumption pattern in Jordan with the assumption that this load is similarly maintained throughout the complete year [5]. As part of a generic RE planning framework in the region, the peak demand is forecasted for the year 2050 using Linear Regression modeling. Accordingly, the peaking demand in 2050 is projected to be

TABLE 2. The predicted cost breakdown of the hybrid energy system in 2050 using typical indicators in Jordan.

Element	Value
Cost of PV system (USD/kW)	323
Annual O&M cost of the PV system (USD/kW)	9.11
Cost of wind system installation (USD/kW)	825
Annual O&M cost of the wind system (USD/kW)	15.73
Cost of Lithium-Ion Battery (USD/kWh)	150
System lifespan (year)	25
Grid electricity cost (USD/kWh)	0.05
Discount Rate (%)	5
Averaged rates	

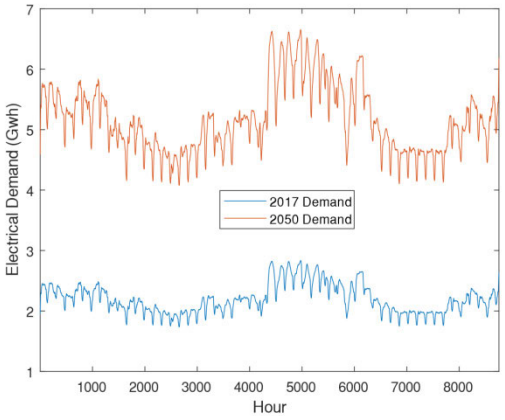

FIGURE 3. Typical hourly energy demand in Jordan during 2017, and 2050 projection.

around 7.67 GWh and the aggregated demand is approximately 45.19 TWh. These projections are consistent with peak energy forecasts of the National Electric Power Company (NEPCO), for the same time. Fig. 3 illustrates the hourly demand for 2017 and the projected demand in 2050.

F. OPTIMIZATION MODEL

Multi-objective optimization involves minimizing or maximizing multiple objective functions. Two solvers in the global optimization toolbox for multi objective optimization: gamultiobj which is based on the genetic algorithm and ParetoSearch which has a pattern search algorithm. Instead of finding a single solution to a single objective function, these solvers find points on the pareto front. This means the points of one objective cannot be improved without hurting the other one. ParetoSearch takes many fewer function evaluations than Genetic Algorithm. Moreover, in both objective function space and decision variable space, the ParetoSearch approach has more points that are closer to the true solution. It should be noted that with control variables that are large the gamultiobj can fail, while ParetoSearch is more vigorous to such condition. Therefore, the present work uses a pattern search algorithm to optimize the installed capacity of components of the RES. The optimization model is based on the ParetoSearch modeling tool in MATLAB and the method has been validated in [59]. The optimization model in this study

TABLE 3. A brief description of the parameters involved in the optimization problem.

Optimization Problem Component	Decision Variables
Without ESS	RES capacities
With ESS	RES and battery capacities
Objective Functions	Minimizing LCOE while Maximizing F_R and DSF
Constraint	LCOE ≤ COE

considers optimizing the capacity of the components of the RES for a single location over 1049 equally spaced points in terms of latitude and longitude. The first objective of this optimization problem is to maximize both the RES fraction relative to grid injection and the demand-supply fraction which are computed as follows,

$$F_{RES} = \frac{D_{RES}}{\mathrm{D}} \tag{27}$$

$$DSF = \frac{H}{\mathrm{T}} \tag{28}$$

The LCOE of the hybrid energy system is modeled as a constraint in this optimization problem, in which the cost of energy generation by the RES can only be equal to or less than the existing grid electricity price. This constraint helps in identifying the economically feasible, and in some cases profitable, scenarios of the RES. After identifying the optimal scenarios, the price constraint is removed for the sake of comparison between optimal and non-optimal results. Table 3 summarizes the input parameters, objectives, and constraints of the optimization problem.

For comparison purposes and to assess the technical performance of the RES system, the annual capacity factor is used which can be estimated as follows:

$$CF = \frac{E_{gen}}{(\mathrm{P_{e,R}} \times N + P) \times 365 \times 24} \tag{29}$$

III. RESULTS AND DISCUSSION

The energy demand-supply mismatch is one of the greatest challenges to the wide disposition of RESs. This is a result of the fluctuating nature of renewable resources. The assessment of resources in literature is usually based on the quantity of the available energy, where the deficit is supplied by an ESS. However, this methodology usually results in a greater deficit portion and larger ESS, as not only the amount of energy that can be produced is important, but its production in times of demand is an important factor as well. Therefore, in this work, we used the demand-supply matching; represented by the RES fraction and DSF, as one objective of the optimization algorithm, while keeping the LCOE at a minimum as a conflicting objective. To do so, Jordan was divided into equally spaced longitudes and latitudes, and the resources were scanned for maximum matching with the forecasted demand; to assess places of highest potential. As such, it is stressed again that the site of the highest potential is considered the one with the highest matching rather than with

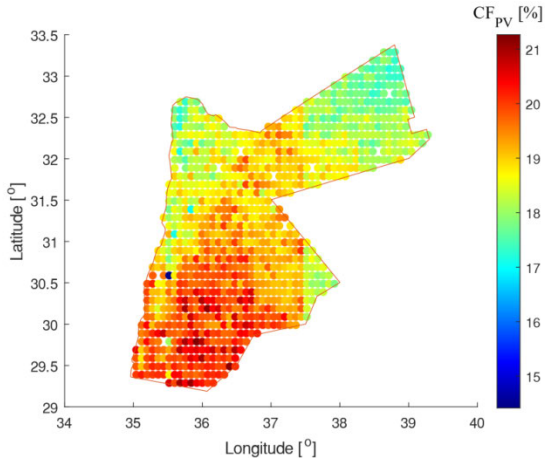

FIGURE 4. Annual capacity factor map of the PV system in Jordan.

the highest energy quantity (solar insolation/wind speeds). First, a standalone PV system without energy storage is considered at each location in Jordan, and the techno-economic performance of the systems is presented. Standalone wind systems without an ESS are then assessed, after which the performance of both systems, PV and wind with an ESS are investigated. Finally, a scenario is set up where the system is comprised of PV and wind units, with and without an ESS at each location. The following subsections present the results in the mentioned order.

A. STANDALONE PV AND WIND SYSTEMS WITHOUT ESS

1) STANDALONE PV SYSTEMS

The performance of the PV systems varies from one location to another because of the uncertainty associated with solar resources as shown in Fig. 4. The variation of the annual capacity factor is relatively small (the majority are between 18% and 21%); however, this could affect the techno-economic aspects of the system, as well as the optimal PV system capacities with almost no effect on the energy production profile since almost all the locations in Jordan, have the same resources profile. Fig. 5 includes a pictorial depiction of the optimal standalone PV system capacities and the corresponding technical and economic parameters in the target case study.

Generating the figure, the LCOE was constrained to the current value in Jordan of 0.05 USD/kWh. This means that the optimal capacities and all other techno and economic parameters were evaluated for feasible systems that can compete in the current market. Since renewable prices are expected to go lower with higher production and fossil fuel prices rise as they become scarce in the next decades, the COE will not dip lower than the current value, therefore, setting it as a constraint represents a conservative limit. Later in Table 4, we show that prioritizing the maximization of the RES fraction and DSF without constraining the LCOE, will not yield much better outcomes in terms of demand met.

TABLE 4. The optimum location, size, and economic requirements of the stand-alone PV system.

Element	Considering LCOE Constraint	Without considering LCOE Constraint
Longitude and Latitude (°)	35.76, 29.5889	36.48,31.1889
PV Capacity (GW)	29.36	58.73
RES Fraction (%)	43.59	45.95
DSF (%)	37.26	41.95
CF (%)	20.58	19.69
Cost of Energy (USD/kWh)	0.0477	0.0906
Net present value (10^9 USD)	2.41	4.5
Payback (years)	3.99	4.19

As illustrated in Fig. 5(a), the capacity of the feasible PV system varies significantly (by almost 10 GW) from one location to another to achieve almost the same RES fraction (around 42%) with a slight change in the DSF (between 32% to 38%). On the other hand, there is significant variation in the LCOE, PBP, and the NPV caused by the solar resources' intensity variation. The optimum location of the PV system that considers maximum RES fraction and DSF (LCOE constrained) is located at Southern Jordan in Ma'an governorate, which is consistent with the results reported in the body of literature [5]. Next, Table 4 shows the parameters of standalone PV systems that exhibit the maximum RES fraction and DSF (with and without a constraint on the LCOE). It is clear from the table that a standalone PV at a single location cannot independently meet the energy load in that particular location, where the maximum achievable RES fraction and DSF even without LCOE constraint were 45.95% and 41.95% respectively. This is an expected consequence of the supply-demand mismatch profiles. Subsequently, the same analysis is conducted for a standalone wind system at a single location.

2) STANDALONE WIND SYSTEMS

Unlike solar resources, wind resources differ dramatically from one location to another which can be seen in the capacity factor variation shown in Fig. 6 (almost between 10% and 55%). This is also reflected in the techno-economic feasibility of these systems and the optimal standalone wind capacities as shown in Fig. 7.

As can be depicted from Fig. 7(a), the feasible wind system optimal capacity varies significantly (by almost 15 GW) from one location to another. Unlike the PV system, there are several locations of unfeasible wind systems where the optimal capacity values are shown as zero (a zero-capacity value represents a point where no feasible optimal solution could be achieved via the optimization algorithm due to the very low site resources). Moreover, the wind systems in the eastern strip of Jordan had the lowest technical and economic performance, while the remaining locations had small variations in the RES fraction (between 70% and 80%) as shown in Fig. 7(d). However, a larger DSF variation in the same

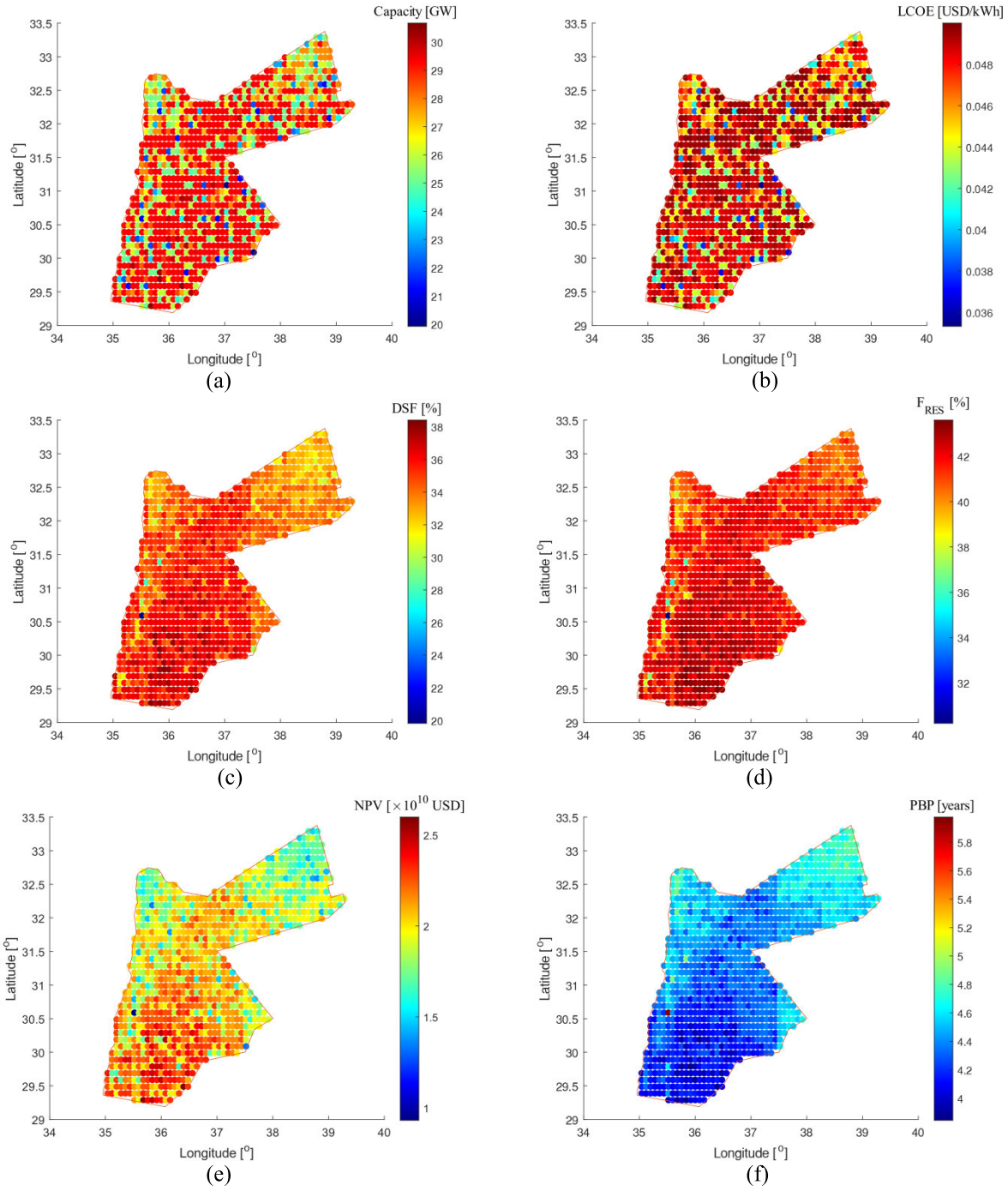

FIGURE 5. Geographical illustration of the optimum capacity of the standalone PV system and the corresponding configurations: a) optimal PV capacity, b) LCOE, c) DSF, d) RES fraction, e) NPV, and f) PBP.

region was calculated (between 40% and 75%). The DSF is more sensitive to supply-demand matching, which illustrates the importance of including these parameters in the sizing problem. The optimum configuration of the independent stand-alone wind turbine (considering LCOE restriction) that has the maximum RES fraction and DSF is found at Northern Jordan in the Mafraq governorate. Table 5 shows the optimum capacity of the standalone wind turbine in the area with its location and reports the corresponding optimum economic requirements. Shown in Table 5, the techno-economic performance of a standalone wind turbine maximizing the RES fraction and DSF without LCOE constraint. It is shown that such a system could cover a significant part of the demand in Jordan, however, its size would be very large and with

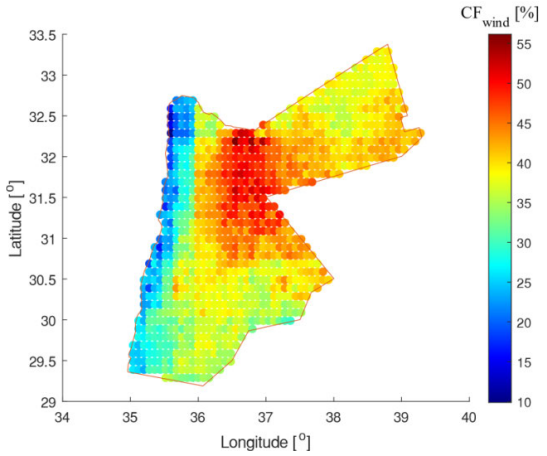

FIGURE 6. Yearly capacity factors of wind turbines in Jordan.

TABLE 5. The optimum location, size, and economic requirements of a stand-alone wind system.

Element	Considering LCOE Constraint	Without considering LCOE Constraint
Longitude and Latitude (°)	36.88, 32.1889	36.48, 30.8889
Wind Capacity (GW)	25.95	536770.07
RES Fraction (%)	85.85	97.78
DSF (%)	75.11	97.56
CF (%)	53.92	46.72
Cost of energy (USD/kWh)	0.0497	90.22
Net present value (10^{10} USD)	5.92	9862.8
Payback (years)	3.74	4.37

unfeasible costs. Therefore, next, standalone wind and PV systems with an integrated ESS will be investigated.

B. STANDALONE PV AND WIND SYSTEMS WITH ESS

Standalone PV systems have usually low technical feasibility compared with other RE resources, due to the nature of solar energy where it is only available during daylight. Therefore, the integration of an ESS to allocate excess energy during the daylight to meet the energy deficit during the night becomes significant. The high capital cost of ESS is the main barrier to their deployment; however, in 2050 National Renewable Energy Laboratory (NREL) predicts that the energy storage cost will decrease by almost half which would make the installation of ESS with RES more feasible.

1) STANDALONE PV SYSTEMS WITH LITHIUM-ION BATTERY BANK

The adaptation of the LIB storage system with the existing PV system significantly increases its technical feasibility where it almost doubled the fractions with LCOE <=0.05 USD/kWh. However, it also doubled the PBP of the system and decreased

TABLE 6. The optimum location, size, and economic requirements of the PV-LIB system.

Element	Considering LCOE Constraint	Without considering LCOE Constraint
Longitude and Latitude (°)	35.92, 29.2889	37.2, 29.9889
PV Capacity (GW)	33.55	96.65
Lithium-Ion Battery Capacity (GWh)	100.66	98.27
RES Fraction (%)	99.55	99.953
DSF (%)	99.304	99.943
CF (%)	20.29	19.36
Cost of energy (USD/kWh)	0.0477	0.0917
Net present value (10^{10} USD)	1.18	5.72
Payback (years)	9.69	6.28

TABLE 7. The optimum location, size, and economic requirements of the wind-LIB system.

Element	Considering LCOE Constraint	Without considering LCOE Constraint
Longitude and Latitude (°)	36.72, 32.2889	36.32, 30.8889
Wind Capacity (GW)	23.88	43.81
Lithium-Ion Battery Capacity (GWh)	25.42	132.14
RES Fraction (%)	92.26	100
DSF (%)	87.61	100
CF (%)	49.85	44.41
Cost of energy (USD/kWh)	0.049	0.1031
Net present value (10^{10} USD)	4.47	5.44
Payback (years)	4.86	7.14

the NPV by almost half due to the increase in the PV and LIB capacities required to increase the demand-supply matching, as shown in Fig. 8. besides, the inclusion of the LIB allowed increasing the number of feasible PV capacities by almost double due to the revenues gained from such integration. It is illustrated that in the governorate Ma'an (south of Jordan) the installed PV system and LIB capacities were less than other locations and at the same time, they had the largest RES and DSF fractions because of the high potential of solar resources in that region. As aforementioned, the optimal PV/LIB (considering LCOE restriction) with the maximum RES and DSF fractions is found in the Ma'an governorate as shown in Table 6. The table shows that when the battery storage was integrated into the PV system, even with a constrain on the LCOE, the RES fraction and DSF achieved were higher than 99%, compared to about 43% before ESS integration. Next, the effect of such integration on the standalone wind system is investigated.

2) STANDALONE WIND SYSTEMS WITH LITHIUM-ION BATTERY BANK

Like the case of PV systems, the usage of LIB enhanced the supply-demand matching by utilizing the excess energy produced to meet the deficit using the ESS, which can be seen by the enhancement in the RES and DSF fractions as shown

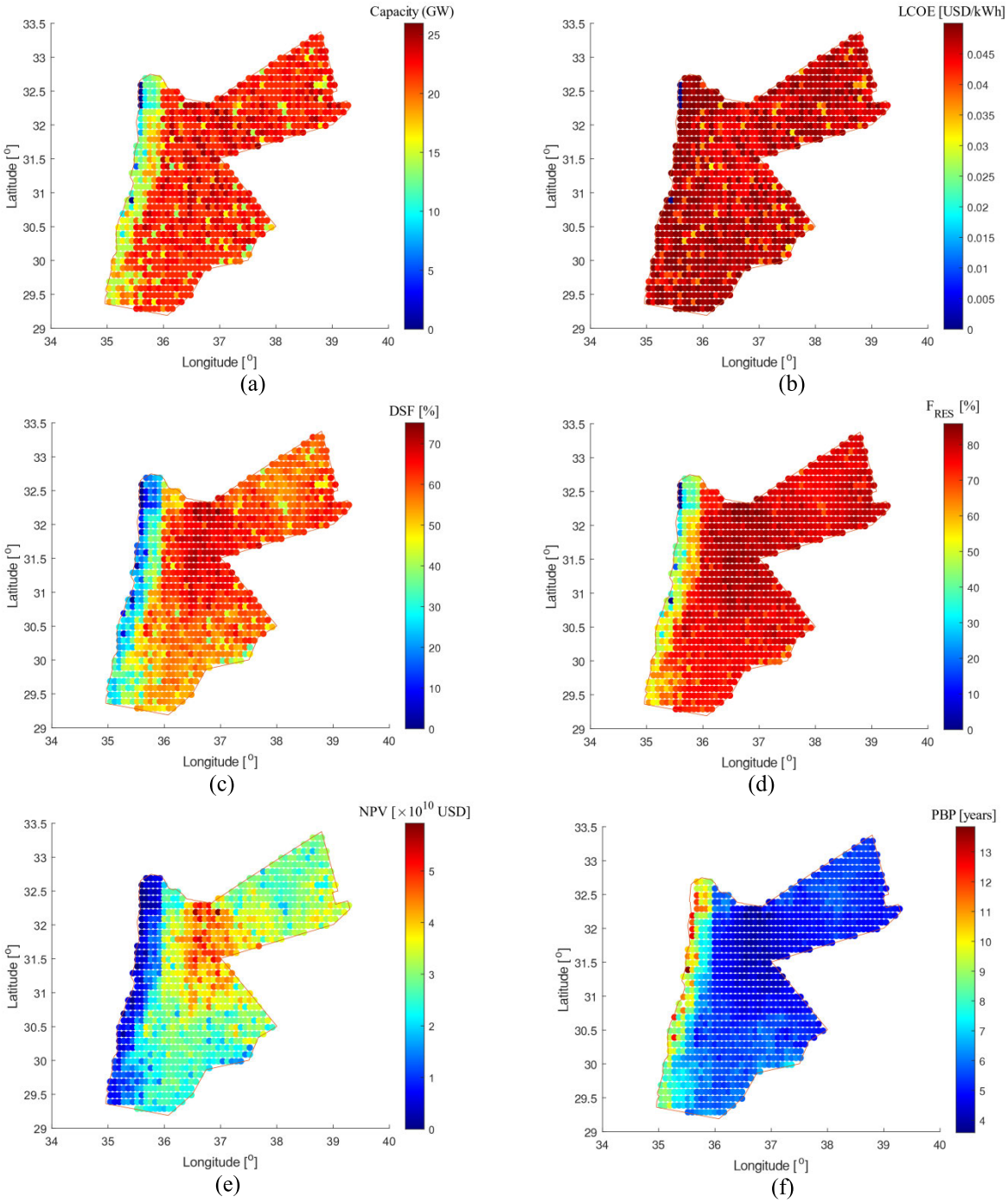

FIGURE 7. Geographical illustration of the optimum capacity of the standalone wind system and the corresponding configurations: a) optimal wind capacity, b) LCOE, c) DSF, d) RES fraction, e) NPV, and f) PBP.

in Fig. 9. However, unlike the case of PV systems, using LIB did not lead to an increment in feasible wind sizes. Further, the increase in RES and DSF fractions is less than that which occurred in LIB integrated PV systems. On the contrary, this integration led to a decrease in the feasible capacities in some regions. Furthermore, the effect of wind-LIB integration on the NPV and the PBP followed a similar trend to that of the PV-LIB integration, but the change was not as significant. It can be seen in Fig. 9 (d) and (e) that the optimal location for wind/LIB (considering LCOE restriction) which has the maximum RES and DSF fractions is optimally found on the Northern part of Jordan in Mafraq governorate at almost the same place for the standalone wind system without ESS as reported in Table 7.

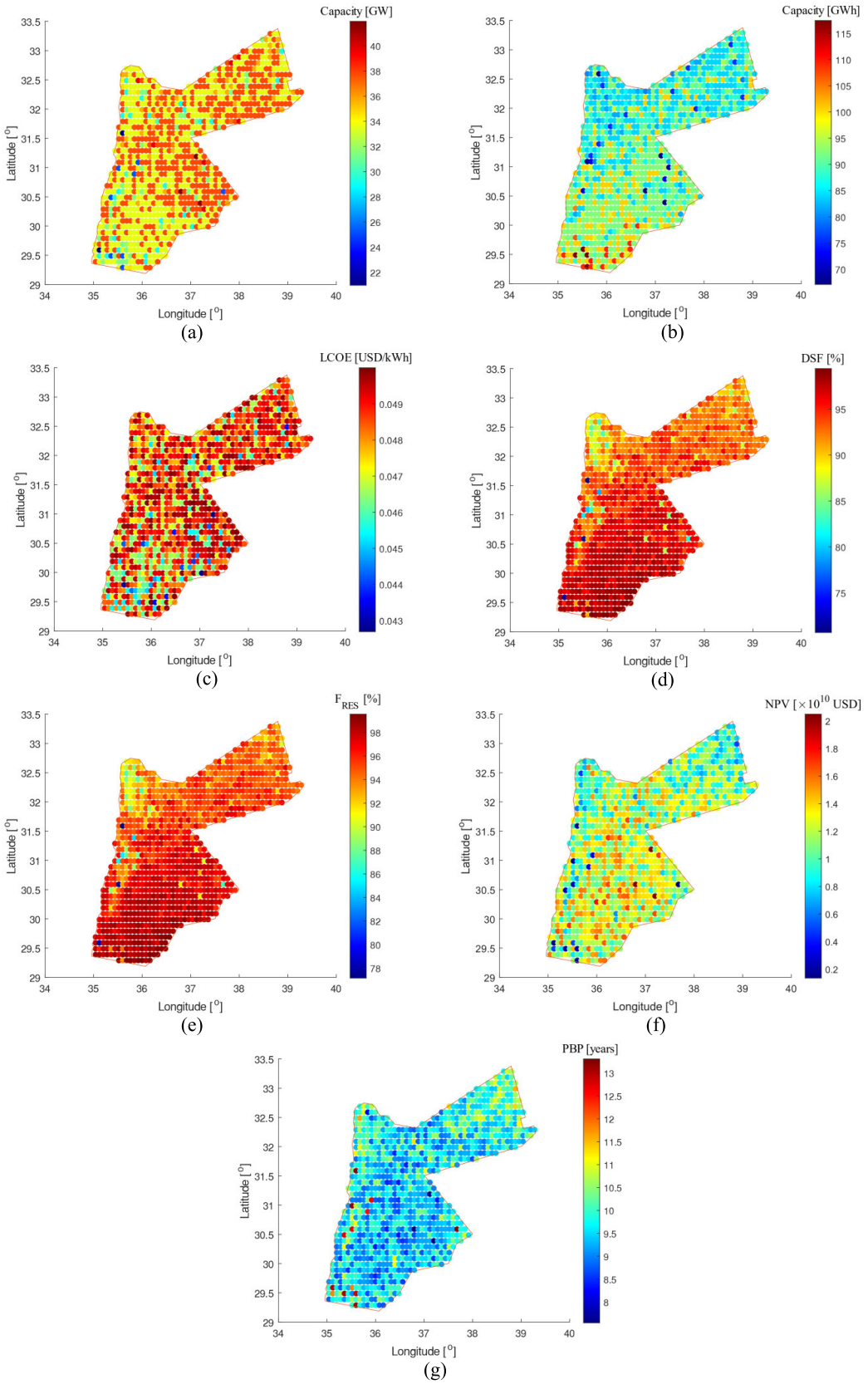

FIGURE 8. Geographical illustration of the optimum capacity of the PV-LIB system and the corresponding configurations: a) optimal PV capacity, b) LCOE, c) DSF, d) RES fraction, e) NPV, and f) PBP.

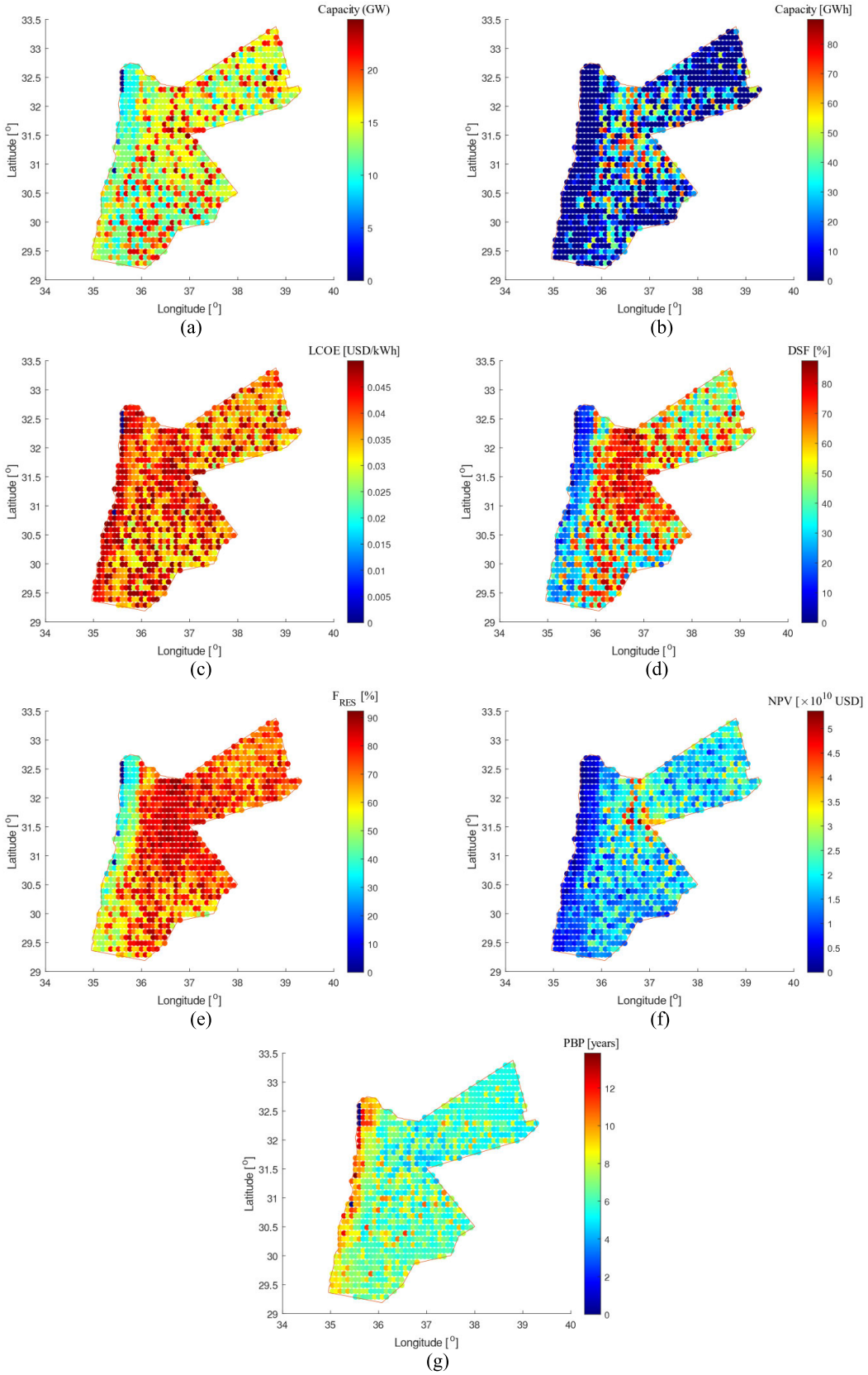

FIGURE 9. Geographical illustration of the optimum capacity of the wind-LIB system and the corresponding configurations: a) optimal wind capacity, b) LCOE, c) DSF, d) RES fraction, e) NPV, and f) PBP.

TABLE 8. The techno-economic aspect of the optimal PV-Wind and hybrid models integrated with an ESS with a constrained LCOE.

Parameter	PV with ESS	Wind with ESS	Hybrid with ESS
Longitude and Latitude (°)	35.92, 29.2889	36.72, 32.2889	36.48, 29.8889
RES Capacity (GW)	33.55	23.88	25.17(PV)+8.2(Wind)
LIB Capacity (GWh)	100.66	25.42	75.5
RES Fraction (%)	99.55	92.26	99.82
DSF (%)	99.304	87.61	99.67
CF (%)	20.29	49.85	25.10
LCOE (USD/kWh)	0.0477	0.049	0.0492
NPV (10^10 USD)	1.18	4.47	2.044
PBP (years)	9.69	4.86	7.92

It can be depicted that the feasible integration of the LIB with the wind system (with LCOE $\leq$ COE), achieved only 92.26% RES fraction and 87.61% DSF which is lower than the ones achieved by the PV/LIB system. The main reason behind this is that the feasible LIB capacity that can be integrated with the wind system is almost four times less than the feasible LIB capacity in the PV system scenario. On the other hand, notice that the unconstrained optimization of the wind/LIB system achieved 100% RES fraction and DSF with less installed capacities and LCOE compared with the unconstrained PV/LIB scenario that could not reach 100%.

C. THE OPTIMAL PV-WIND HYBRID SYSTEM WITH AND WITHOUT AN ESS: LOCATION AND TECHNO-ECONOMIC PERFORMANCE

Along with the ESS, the hybridization of renewable resources has been widely used to increase the energy profile matching of the resources and demand. Therefore, in this subsection, we have investigated the technical and economic aspects of the hybrid model, with and without energy storage to compare the hybrid resources potential with standalone systems. Fig. 10 presents the optimal hybrid system without an ESS techno-economic performance and location, and with a constrained LCOE. In contrast, Fig. 11 presents the case for when the system is integrated with an ESS with and without a constraint on the LCOE. The optimal hybrid system without an ESS was able to achieve a RES fraction of 90.6% with PV and wind capacities equal to 18.9 GW and 18.4 GW respectively, even without an ESS. This is far superior to the previously achieved value of 70% by Kiwan and Al-Gharibeh [5], which shows that resource assessment should be based on the ability of the RES in a certain area to match the demand rather than scanning for areas of highest wind speeds or solar insolation. When the LCOE constraint was removed, the system could achieve a RES fraction of 99.45%, however, the system was extremely large and unrealistic, therefore, was not included.

When an ESS was integrated into this particular hybrid model, 99.8% of the demand was met at a constrained LCOE.

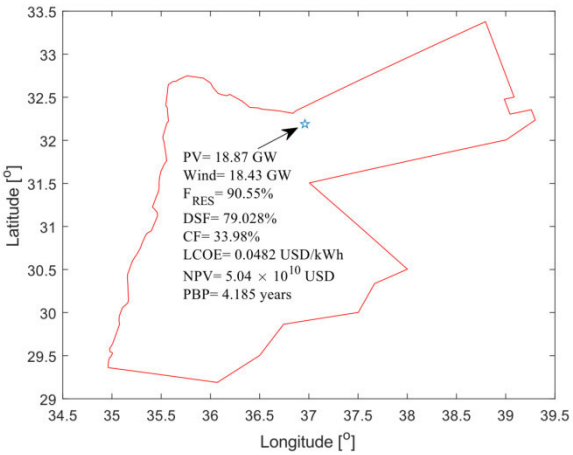

FIGURE 10. The optimum capacities of the PV-wind hybrid model and the respective locations as well as the economic parameters with LCOE constraints.

It's worth noting that in the latter case, the DSF was also much higher than when no ESS was used; namely, 99.7% compared to 79%. Additionally, without a constraint on LCOE, the hybrid model with an ESS could always achieve 100% of the demand, with a comparable LCOE of 0.06 USD/kWh compared to the constrained LCOE of 0.05 USD/kWh. Since the prices of renewable technologies are expected to significantly decline in the upcoming decades, this final case could become the most appealing.

Finally, for the sake of side by side comparison, Table 8 shows the optimal cases of the three scenarios, i.e. standalone PV, standalone Wind, and hybrid system, when they were integrated into an ESS and the LCOE constraint was forced. Note that both PV and hybrid systems could achieve very high RES fraction and DSF, i.e. >99%, with a comparable system's capacity. However, the hybrid system led to a 25% reduction in the size of the ESS. Also, the payback period of both systems is comparable. On the other hand, the constrained LCOE wind system achieved lower RES fraction and DSF of 92.3% and 87.6% respectively, but it also had a small-sized ESS. The prices of wind technology and constraint forced on the LCOE makes it difficult for it to

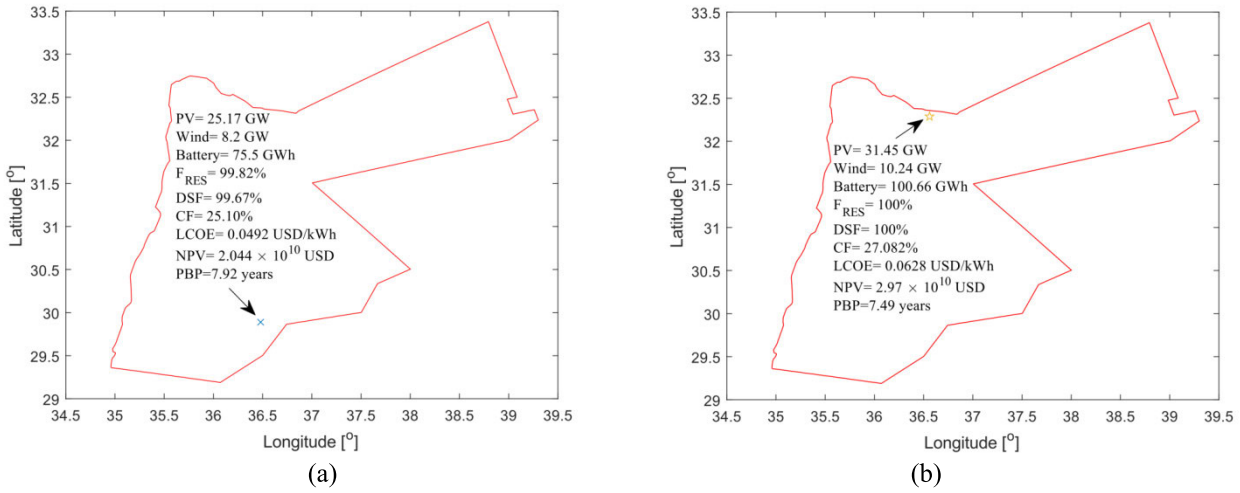

FIGURE 11. The optimal RES capacities (PV, wind, and battery) and the respective location in addition to the techno-economic parameters with LCOE: a) constraint and b) without constraint.

compete in this presented scenario. However, when the LCOE constraint was removed, the standalone wind with ESS was able to achieve a RES fraction and DSF of 100%, with a 33% larger system's and ESS capacities and almost double the LCOE. As the prices of wind technology drop in the future, its competitiveness and portion of the RES fraction to supply the energy demands can significantly improve.

IV. CONCLUSION

This study presents a new approach to assess the solar and wind resources potential in the countries based on the matching between the demand and the supply which would ensure the maximum and the most efficient utilization of these resources. The optimal RES capacities with and without ESS were found at each location using multi-objective optimization based on maximizing the RES fraction and the demand-supply fraction while minimizing the LCOE. Several RES configurations have been considered while mapping the performance considering a real-world test system. The proposed approach was used to map the techno-economic feasibility of the solar and wind resources in Jordan as a case study noting that this approach can be applied to any location.

The results in this study showed that mapping RE resources help to identify the best locations that possess the highest matching between the electricity generation and the demand profiles in Jordan. Furthermore, the results show that two RES configurations can almost cover the whole demand in Jordan with LCOE less than the local cost of electricity: namely, PV/LIB and PV/wind/LIB systems. This PV/LIB system consists of 33.55 GW PV capacity, 100.66 GWh LIB and has LCOE of 0.0477 USD/kWh, while the PV/wind/LIB consists of 25.17 GW PV capacity, 8.2 GW wind capacity, 75.5 GWh LIB and has LCOE of 0.0492 USD/kWh. Finally, the mapping approach presented in this study enabled a RES fraction of 90.6% to be achieved without an ESS, compared to 70% previously reported which was based on the installation at sites of appealing energy quantities rather than matching; demonstrating the superiority of the presented approach. A smart optimized framework for the effective operation of RE systems has to be introduced as a future research direction.

NOMENCLATURE

SYMBOLS

A_m	PV panel area, m^2
C_{ESS}	systems capital cost, USD
C_i	RES capital cost, USD
C_{PV}	Cost of PV system installation, USD
C_{WT}	Cost of the wind system installation, USD
CF	Annual RES capacity factor, %
COE	Electricity cost E, USD/kWh
D	Electrical demand, kWh D_E Surplus energy, kWh
D_{Gr}	Electricity consumed from grid, kWh
D_{RES}	Energy consumption supplied at t time by the RES, kWh
DOC	ESS depth of charge, kWh
DSF	Yearly electrical demand to supply ratio, %
E_G	Total electricity generated by the RES, MWh
E_{PV}	Electric power generation by PV plant, kWh
E_{St}	Electricity stored in the ESS at time t, kWh
E_{wind}	Energy generated by the wind turbine, kWh
F_{RES}	Annual RES fraction, %
H	Number of grid-independent hours in a year
$I_{b,n}$	Hourly direct radiation, Wh/m^2
$I_{b,t}$	Hourly direct radiation on an inclined surface, Wh/m^2
I_d	Hourly diffuse radiation, Wh/m^2
$I_{d,t}$	Hourly diffuse radiation on an inclined surface, Wh/m^2
I_{Ref}	PV module reference radiation, Wh/m^2

I_T	Total radiation incident on an inclined surface, Wh/m^2
K	Weibull distribution shape coefficient
LT	RES lifespan, years
L_{loc}	Longitude, °
L_{st}	Standard meridian, °
LCOE	Levelized cost of electricity, USD/kWh
M_t	Annual O&M cost, USD
N	Wind turbines total number
N_m	PV plant modules total number
NOCT	PV nominal temperature, °C
NPV	Net present value, USD
n	Number of days in one year
P	PV system capacity, kW
P_e	Hourly electrical power generated by the wind system, kW
$P_{e,R}$	Nominal electric wind turbine power, kW
PR	PV system performance ratio, %
PBP	Payback period, years
R_t	Annual profit gained by the RES, USD
R_{t1}	Profit gained by the RES in the first year, USD
r	Yearly Discount rate, %
T_{amb}	Ambient temperature, °C
T_{PV}	PV cell temperature, °C
$T_{Ref,NOCT}$	PV temperature at nominal test conditions,°C
T_{RefSTC}	PV temperature at standard test conditions, °C
T_z	Local time zone, hour
t	Number of hours in a period
t_s	Solar time, hour
t_{std}	Local time, hour
u_C	Cut-in wind speed, m/ s
u_F	Cut-out wind speed, m/s
u_R	Rated wind speed of the turbine, m/s
u_z	Wind Speed at hub height, m/s
u_1	Average wind speed at 10m, m/s
$\bar{u}$	Mean wind speed at hub height, m/s
Z	Hub height, m
Z_1	Ground-level elevation, m/s

ACRONYMS AND ABBREVIATIONS

COE	Cost of electricity
DSF	Demand Supply Fraction Energy storage system
JEPCO	Jordan Electric Power Company
O&M	Operation and Maintenance
RE	Renewable Energy
RES	Renewable Energy System
NPV	Net Present Value
PBP	Simple payback period Photovoltaic
PV	Photovoltaic

GREEK LETTERS

α	Wind shear coefficient
β	The inclination angle of the PVpa
β_{Ref}	PV temperature coefficient, 1/°C
γ	Surface azimuth angle, °
γ_s	Solar azimuth angle, °
δ	Declination angle, °
η_{PV}	PV panel efficiency, %
$\eta_{PV,\,Ref}$	Reference efficiency of the PV panel, %
θ	The angle of incidence, °
θ_z	Zenith angle, °
σ	wind speeds standard deviation, m/s
ϕ	Latitude angle, ° Hour angle, °
ω	Hour angle, °

REFERENCES

[1] R. M. Elavarasan, G. Shafiullah, K. Raju, V. Mudgal, M. T. Arif, T. Jamal, S. Subramanian, V. S. S. Balaguru, K. S. Reddy, and U. Subramaniam, "COVID-19: Impact analysis and recommendations for power sector operation," *Appl. Energy*, vol. 279, Dec. 2020, Art. no. 115739.

[2] B. Gardiner. (2020). *How Renewable Energy Could Emerge on Top After the Pandemic*. [Online]. Available: https://e360.yale.edu/features/how-renewable-energy-could-emerge-on-top-after-the-pandemic?fbclid=IwAR3I-EH3vsCRm6KPJBCDfOFSowo3WfIfqfSlbbizKFseFbz4_2Ym5qzrBG0

[3] D. Deb, A. Dixit, and L. Chandra, Eds., *Renewable Energy and Climate Change: Proceedings of Rec 2019*. Singapor: Springer Verlag, 2020, doi: 10.1007/978-981-32-9578-0.

[4] G. Abu-Rumman, A. I. Khdair, and S. I. Khdair, "Current status and future investment potential in renewable energy in jordan: An overview," *Heliyon*, vol. 6, no. 2, Feb. 2020, Art. no. e03346.

[5] S. Kiwan and E. Al-Gharibeh, "Jordan toward a 100% renewable electricity system," *Renew. Energy*, vol. 147, pp. 423–436, Mar. 2020.

[6] P. Patel, A. Shandilya, and D. Deb, "Optimized hybrid wind power generation with forecasting algorithms and battery life considerations," in *Proc. IEEE Power Energy Conf. Illinois (PECI)*, Feb. 2017, pp. 1–6.

[7] T. Muneer, M. Asif, and S. Munawwar, "Sustainable production of solar electricity with particular reference to the indian economy," *Renew. Sustain. Energy Rev.*, vol. 9, no. 5, pp. 444–473, Oct. 2005.

[8] E. S. Hrayshat, "Analysis of renewable energy situation in Jordan," *Renew. Sustain. Energy Rev.*, vol. 11, no. 8, pp. 1873–1887, Oct. 2007.

[9] F. Derakhshan, *On Sustainability in Local Energy Planning*. Lund, Sweden: Lund Univ., 2011.

[10] D. Kapoor, P. Sodhi, and D. Deb, "A novel control strategy to simulate solar panels," in *Proc. Int. Conf. Signal Process. Commun. (SPCOM)*, Jul. 2012, pp. 1–5.

[11] R. K. Dhar, A. Merabet, A. Al-Durra, and A. M. Y. M. Ghias, "Power balance modes and dynamic grid power flow in solar PV and battery storage experimental DC-link microgrid," *IEEE Access*, vol. 8, pp. 219847–219858, 2020.

[12] G. Kahen, "Integrating energy planning and techno-economic development: A solid basis for the assessment and transfer of energy technology to developing countries," *Energy Sources*, vol. 20, nos. 4–5, pp. 343–361, 1998.

[13] G. Papaefthymiou and K. Dragoon, "Towards 100% renewable energy systems: Uncapping power system flexibility," *Energy Policy*, vol. 92, pp. 69–82, May 2016.

[14] P. Patel and D. Deb, "Battery state of charge based algorithm for optimal wind farm power management," in *Proc. 6th Int. Conf. Comput. Appl. Electr. Eng.-Recent Adv. (CERA)*, Oct. 2017, pp. 42–46.

[15] X. Yue, N. Patankar, J. Decarolis, A. Chiodi, F. Rogan, J. P. Deane, and B. O'Gallachoir, "Least cost energy system pathways towards 100% renewable energy in Ireland by 2050," *Energy*, vol. 207, Sep. 2020, Art. no. 118264.

[16] A. Azzuni, A. Aghahosseini, M. Ram, D. Bogdanov, U. Caldera, and C. Breyer, "Energy security analysis for a 100% renewable energy transition in Jordan by 2050," *Sustainability*, vol. 12, no. 12, p. 4921, Jun. 2020.

[17] H. Lund and B. V. Mathiesen, "Energy system analysis of 100% renewable energy systems—The case of denmark in years 2030 and 2050," *Energy*, vol. 34, no. 5, pp. 524–531, May 2009.

[18] G. S. Seck, V. Krakowski, E. Assoumou, N. Maïzi, and V. Mazauric, "Embedding power system's reliability within a long-term energy system optimization model: Linking high renewable energy integration and future grid stability for France by 2050," *Appl. Energy*, vol. 257, Jan. 2020, Art. no. 114037.
[19] M. Rezaei, K. R. Khalilpour, and M. A. Mohamed, "Co-production of electricity and hydrogen from wind: A comprehensive scenario-based techno-economic analysis," *Int. J. Hydrogen Energy*, Apr. 2021, doi: 10.1016/j.ijhydene.2021.03.004.
[20] X. Yao, B. Yi, Y. Yu, Y. Fan, and L. Zhu, "Economic analysis of grid integration of variable solar and wind power with conventional power system," *Appl. Energy*, vol. 264, Apr. 2020, Art. no. 114706.
[21] D. Kapoor, P. Sodhi, and D. Deb, "Solar panel simulation using adaptive control," in *Proc. IEEE Int. Conf. Control Appl.*, Oct. 2012, pp. 1124–1130.
[22] Y. Yoo and G. S. J. Jung, "A study on sizing of substation for PV with optimized operation of BESS," *IEEE Access*, vol. 8, pp. 214577–214585, 2020.
[23] B. Bhandari, K.-T. Lee, C. S. Lee, C.-K. Song, R. K. Maskey, and S.-H. Ahn, "A novel off-grid hybrid power system comprised of solar photovoltaic, wind, and hydro energy sources," *Appl. Energy*, vol. 133, pp. 236–242, Nov. 2014.
[24] Y. Zhang, J. Ren, Y. Pu, and P. Wang, "Solar energy potential assessment: A framework to integrate geographic, technological, and economic indices for a potential analysis," *Renew. Energy*, vol. 149, pp. 577–586, Apr. 2020.
[25] R. Rabbani and M. Zeeshan, "Exploring the suitability of MERRA-2 reanalysis data for wind energy estimation, analysis of wind characteristics and energy potential assessment for selected sites in Pakistan," *Renew. Energy*, vol. 154, pp. 1240–1251, Jul. 2020.
[26] A. Rezaeiha, H. Montazeri, and B. Blocken, "A framework for preliminary large-scale urban wind energy potential assessment: Roof-mounted wind turbines," *Energy Convers. Manage.*, vol. 214, Jun. 2020, Art. no. 112770.
[27] M. Al-Nimr, S. Kiwan, and H. Sharadga, "A hybrid TEG/wind system using concentrated solar energy and chimney effect," *Int. J. Energy Res.*, vol. 42, no. 7, pp. 2548–2563, Jun. 2018.
[28] H. S. Dhiman, P. Anand, and D. Deb, "Wavelet transform and variants of SVR with application in wind forecasting," in *Innovations in Infrastructure*. Singapore: Springer, 2019, pp. 501–511.
[29] M. Mostafa, H. M. Abdullah, and M. A. Mohamed, "Modeling and experimental investigation of solar stills for enhancing water desalination process," *IEEE Access*, vol. 8, pp. 219457–219472, 2020.
[30] M. A. H. El-Sayed and J. Kreusel, "Substitution potential of solar thermal power stations in electrical energy systems," *Renew. Energy*, vol. 6, no. 7, pp. 849–854, Oct. 1995.
[31] F. Blaabjerg and K. Ma, "Future on power electronics for wind turbine systems," *IEEE J. Emerg. Sel. Topics Power Electron.*, vol. 1, no. 3, pp. 139–152, Sep. 2013.
[32] C. L. Archer, "Evaluation of global wind power," *J. Geophys. Res.*, vol. 110, no. D12, 2005, Art. no. D12110.
[33] A. M. Foley, P. G. Leahy, A. Marvuglia, and E. J. McKeogh, "Current methods and advances in forecasting of wind power generation," *Renew. Energy*, vol. 37, no. 1, pp. 1–8, Jan. 2012.
[34] A. D. Ahmad, A. M. Abubaker, Y. S. H. Najjar, and Y. M. A. Manaserh, "Power boosting of a combined cycle power plant in Jordan: An integration of hybrid inlet cooling & solar systems," *Energy Convers. Manage.*, vol. 214, Jun. 2020, Art. no. 112894.
[35] S. Ghosh and I. Dincer, "Development and analysis of a new integrated solar-wind-geothermal energy system," *Sol. Energy*, vol. 107, pp. 728–745, Sep. 2014.
[36] G. C. Yoon, K.-S. Shin, M. K. Gupta, K. Y. Lee, J.-H. Lee, Z. L. Wang, and S.-W. Kim, "High-performance hybrid cell based on an organic photovoltaic device and a direct current piezoelectric nanogenerator," *Nano Energy*, vol. 12, pp. 547–555, Mar. 2015.
[37] N. A. Ahmed, M. Miyatake, and A. K. Al-Othman, "Power fluctuations suppression of stand-alone hybrid generation combining solar photovoltaic/wind turbine and fuel cell systems," *Energy Convers. Manage.*, vol. 49, no. 10, pp. 2711–2719, Oct. 2008.
[38] A. Arabali, M. Ghofrani, M. Etezadi-Amoli, and M. S. Fadali, "Stochastic performance assessment and sizing for a hybrid power system of solar/wind/energy storage," *IEEE Trans. Sustain. Energy*, vol. 5, no. 2, pp. 363–371, Apr. 2014.
[39] M. D. A. Al-falahi, S. D. G. Jayasinghe, and H. Enshaei, "A review on recent size optimization methodologies for standalone solar and wind hybrid renewable energy system," *Energy Convers. Manage.*, vol. 143, pp. 252–274, Jul. 2017.
[40] N. Alshammari and J. Asumadu, "Optimum unit sizing of hybrid renewable energy system utilizing harmony search, Jaya and particle swarm optimization algorithms," *Sustain. Cities Soc.*, vol. 60, Sep. 2020, Art. no. 102255.
[41] L. Al-Ghussain, R. Samu, O. Taylan, and M. Fahrioglu, "Sizing renewable energy systems with energy storage systems in microgrids for maximum cost-efficient utilization of renewable energy resources," *Sustain. Cities Soc.*, vol. 55, Apr. 2020, Art. no. 102059.
[42] M. R. Elkadeem, S. Wang, A. M. Azmy, E. G. Atiya, Z. Ullah, and S. W. Sharshir, "A systematic decision-making approach for planning and assessment of hybrid renewable energy-based microgrid with techno-economic optimization: A case study on an urban community in egypt," *Sustain. Cities Soc.*, vol. 54, Mar. 2020, Art. no. 102013.
[43] A. M. Eltamaly, M. A. Mohamed, and A. I. Alolah, "A novel smart grid theory for optimal sizing of hybrid renewable energy systems," *Sol. Energy*, vol. 124, pp. 26–38, Feb. 2016.
[44] L. Ramirez Camargo, J. Valdes, Y. Masip Macia, and W. Dorner, "Assessment of on-site steady electricity generation from hybrid renewable energy systems in chile," *Appl. Energy*, vol. 250, pp. 1548–1558, Sep. 2019.
[45] F. Al-Turjman and M. Abujubbeh, "IoT-enabled smart grid via SM: An overview," *Future Gener. Comput. Syst.*, vol. 96, pp. 579–590, Jul. 2019.
[46] B. V. Ermolenko, G. V. Ermolenko, Y. A. Fetisova, and L. N. Proskuryakova, "Wind and solar PV technical potentials: Measurement methodology and assessments for russia," *Energy*, vol. 137, pp. 1001–1012, Oct. 2017.
[47] O. Nematollahi, P. Alamdari, M. Jahangiri, A. Sedaghat, and A. A. Alemrajabi, "A techno-economical assessment of solar/wind resources and hydrogen production: A case study with GIS maps," *Energy*, vol. 175, pp. 914–930, May 2019.
[48] A. A. Prasad, R. A. Taylor, and M. Kay, "Assessment of solar and wind resource synergy in Australia," *Appl. Energy*, vol. 190, pp. 354–367, Mar. 2017.
[49] S. Sterl, S. Liersch, H. Koch, N. P. M. V. Lipzig, and W. Thiery, "A new approach for assessing synergies of solar and wind power: Implications for West Africa," *Environ. Res. Lett.*, vol. 13, no. 9, Sep. 2018, Art. no. 094009.
[50] A. M. Eltamaly, M. A. Mohamed, M. S. Al-Saud, and A. I. Alolah, "Load management as a smart grid concept for sizing and designing of hybrid renewable energy systems," *Eng. Optim.*, vol. 49, no. 10, pp. 1813–1828, Oct. 2017.
[51] M. A. Mohamed, T. Jin, and W. Su, "An effective stochastic framework for smart coordinated operation of wind park and energy storage unit," *Appl. Energy*, vol. 272, Aug. 2020, Art. no. 115228.
[52] G. M. Shafiullah, "Hybrid renewable energy integration (HREI) system for subtropical climate in central queensland, australia," *Renew. Energy*, vol. 96, pp. 1034–1053, Oct. 2016.
[53] R. M. Elavarasan, G. M. Shafiullah, S. Padmanaban, N. M. Kumar, A. Annam, A. M. Vetrichelvan, L. Mihet-Popa, and J. B. Holm-Nielsen, "A comprehensive review on renewable energy development, challenges, and policies of leading Indian states with an international perspective," *IEEE Access*, vol. 8, pp. 74432–74457, 2020.
[54] M. Shoeb and G. Shafiullah, "Renewable energy integrated islanded microgrid for sustainable irrigation—A Bangladesh perspective," *Energies*, vol. 11, no. 5, p. 1283, May 2018.
[55] *Annual Report*, J. N. E. P. Company, Auburn Hills, MI, USA, 2019.
[56] *Saudi Arabia and Jordan to Develop Electricity Interconnection Grid*, The National US, Washington, DC, USA, 2020.
[57] J. A. Duffie, W. A. Beckman, and N. Blair, *Solar Engineering of Thermal Processes, Photovoltaics and Wind*. Hoboken, NJ, USA: Wiley, 2020.
[58] L. Al-Ghussain, A. M. Abubaker, and A. Darwish Ahmad, "Superposition of renewable-energy supply from multiple sites maximizes demand-matching: Towards 100% renewable grids in 2050," *Appl. Energy*, vol. 284, Feb. 2021, Art. no. 116402.
[59] L. AL-Ghussain, O. Taylan, and M. Fahrioglu, "Sizing of a photovoltaic-wind-oil shale hybrid system: Case analysis in Jordan," *J. Sol. Energy Eng.*, vol. 140, no. 1, pp. 1–12, Feb. 2018.

LOIY AL-GHUSSAIN received the B.S. degree in mechanical engineering from the University of Jordan, Amman, Jordan, in 2015, and the M.Sc. degree in sustainable environment and energy systems from Middle East Technical University Northern Cyprus Campus, Guzelyurt, Northern Cyprus, in 2017. He is currently pursuing the Ph.D. degree with the University of Kentucky, Kentucky. He worked as a Research Assistant with the Department of Mechatronics Engineering, German Jordanian University, Amman. He worked as a Teaching Assistant with the Mechanical Engineering Department, Middle East Technical University Northern Cyprus Campus. His research interests include stretchable and wearable sensors, microfluidic systems, and renewable energy as well as atmospheric turbulence and small UAVs.

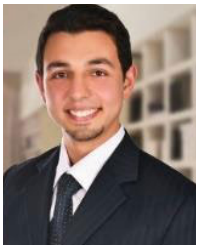

ADNAN DARWISH AHMAD received the B.S. degree in mechanical engineering from the University of Jordan, in 2015, and the M.Sc. degree from the University of Kentucky, where he is currently pursuing the Ph.D. degree. From 2016 to 2021, he was a Research Assistant with the Institute of Research for Technology Development (IR4TD), University of Kentucky and has worked on multiple funded projects, including atomization and sprays, renewable energy and power cycles modeling, and wildland fire research. His research interests include experimental flow visualizations, heat transfer and scale modeling, hybrid energy systems, and fire research.

AHMAD M. ABUBAKER received the B.Sc. and M.Sc. degrees in mechanical engineering from the Jordan University of Science and Technology (JUST), Irbid-Jordan, in 2013 and 2016, respectively. He is currently pursuing the Ph.D. degree with the University of Kentucky, Lexington, KY, USA. From 2013 to 2017, he was a Research Assistant with the Mechanical Engineering Department, JUST. Since 2018, he has been a Research Assistant with the Institute of Research for Technology Development (IR4TD) University of Kentucky and has worked on multiple projects, including atomization and sprays, renewable energy, and power cycles modeling. His research interests include gas turbines, novel condensers, parabolic trough collector's inlet air-cooling, and hybrid energy systems.

MOHAMMAD ABUJUBBEH received the B.Sc. degree in electrical and electronic engineering (power systems) from Eastern Mediterranean University, Famagusta, Cyprus, in 2016, and the M.Sc. degree in sustainable environment and energy systems from Middle East Technical University, Northern Cyprus Campus, in 2019. He is currently pursuing the Ph.D. degree in electrical and computer engineering with Kansas State University. His research interests include cyber-physical systems, renewable energy integration, probabilistic voltage and loss sensitivity analysis, and the IoT-enabled smart grids.

ABDULAZIZ ALMALAQ (Member, IEEE) received the B.S. degree in electrical engineering from the College of Engineering, University of Hail, Hail, Saudi Arabia, in 2011, the M.S. and Ph.D. degrees in electrical engineering from the Department of Electrical and Computer Engineering, University of Denver, Denver, CO, USA, in 2015 and 2019, respectively. He is currently an Assistant Professor with the Department of Electrical Engineering, University of Hail. He published many journal articles at highly ranked ISI journals, and published several conference papers at distinguished conferences. His research interests include modeling smart buildings, smart grids, smart cities, and smart energy systems utilizing artificial intelligence, machine learning, and deep learning. He is the Vice-Chair of the IEEE Saudi Arabia Signal Processing Society Chapter.

MOHAMED A. MOHAMED (Member, IEEE) received the B.Sc. and M.Sc. degrees in electrical engineering from Minia University, Minia, Egypt, in 2006 and 2010, respectively, and the Ph.D. degree in electrical engineering from King Saud University, Riyadh, Saudi Arabia, in 2016. He joined the College of Electrical Engineering and Automation, Fuzhou University, China, as a Postdoctoral Research Fellow, in 2018. Since 2008, he has been a Faculty Member with the Department of Electrical Engineering, College of Engineering, Minia University. He has supervised multiple M.Sc. and Ph.D. theses, worked on a number of technical projects, and published various articles and books. His research interests include power system analysis, renewable energy integration, energy management, power electronics, electrical vehicles, optimization, smart islands, smart cities, and smart grids. He has also joined the editorial board of some scientific journals and the steering committees of many international conferences.